Earthquake Motions Observed on Rock and Ground

By Kojiro IRIKURA and Junpei AKAMATSU

(Manuscript received January 13, 1975)

Abstract

Earthquake motions were observed using an automated seismic recording system with short-period velocity seismometers at rock site and ground site, which are adjacent, on the eastern side of Kyoto basin. The influence of topographic features on the motions at a rock site was studied from examining the nature of particle motions of P and S waves. Amplification factors of the motions at a ground were studied from comparison of spectral characteristics between motions at the rock and those at the ground.

The ratios of the amplitudes of P and S motions at the ground to those at the rock vary appreciably from 0.8 to 8.0 from event to event. The spectral ratios between the ground motions and rock motions show that the frequencies and amplitudes of the peaks are different in dependence of the incident direction of the events.

The causes of the variation of the amplitude ratios is found to be that the amplitudes of the motions at the rock site on the hill, vary with the incident angles and the directions of seismic arrivals. And the peak frequencies of the responses of seismic motions at the ground site, underlied by dipped base rock, are considered to vary with the directions of seismic arrivals.

1. Introduction

It is well known that the earthquake motions on a ground during an earthquake are significantly amplified by the near-surface layering. Amplification factors of seismic waves at a given site might be theoretically calculated, if the physical parameters of the layered media under the ground could be determined[1]. In practice, however, it is difficult to determine the layering and the physical parameters at a site in urban areas by experimental measurements, for example, such as seismic prospecting. And also complexity of local geology and topography in many cases of real grounds will make it difficult to estimate the amplification factors. In this study, as a method of direct estimation of amplification at a ground site, comparison of the earthquake motions observed on rock and ground is attempted.

The first procedure to obtain amplification factors at a given site is to estimate characteristics of incident seismic waves to the bed rock under the ground. In obtaining incident waves from the data observed on a surface outcrop, the relations between the motions at the outcrop and those at the bed rock should be discussed. Because the motions observed on a rock surface are affected not only by the source and propagation path but also by local geology and topography in the vicinity of the site. The spatial extent to which the seismic waves are uniform depends on horizontal heterogeneity of

the geological configuration and wave lengths[2),3)].

The next procedure is to compare the seismic motions on rock and ground and to estimate amplification effects caused by ground structure. Then, the amplitudes of the same wave types between the seismograms on those two sites have to be compared and so identification and separation of the same phases is necessary. Particularly in case of estimation of amplification of S waves' motions, the incident azimuth of seismic waves at each site have to be examined for separation of SH phases and SV phases.

In order to discuss amplification factors due to a ground condition in terms of observable physical parameters, we need to consider observational systems as well as the method of data processing. Recently, observational systems using strong motion accelerographs have been set up at many places, as a direct method for predicting the ground behavior during large earthquakes. However, strong motions experienced by large earthquakes can be seldom recorded at a given site and so reappearence of the same earthquake motions can hardly be expected, even if a strong motion were recorded. Examination of site conditions and extrapolation of characteristics of strong earthquake motions are required to be made, based on seismic data of small earthquakes obtainable for relatively short periods of time.

In our laboratory, a magnetic tape recording system with a drum recorder for time delay was deviced. This system records compactly seismic data in analog form, and observed analog data are easily converted to digital ones using an A–D converter. Observational points for this study are situated on a ground and a rock outcrop, where 3-components short period seismometers have been installed.

In the present paper, the data recording system is described and characteristics of earthquake motions observed on rock and ground are discussed to study methods of estimation of characteristics of rock motions and amplification of ground motions.

2. Observational system

In this study it is desired for the observational system to obtain small earthquake motions i.e., less than intensity II and to record seismic data adequate for digital analysis using electronic computer. The following conditions to design the system were considered; (1) the frequency range upto 25 Hz and the dynamic range of 40 db in SN ratio, (2) routine observation over long periods of time and (3) easy and accurate conversion of analog to digital form. In addition, reliable and compact recording of desired data was required to obtain and analyze a large quantity of data. Magnetic recording system with time delay equipment that incorporates an automatic detector of seismic events is one of the methods to implement these conditions. Furuzawa indicated the merits and the demerits of various instrumentation of the automated seismic recording system and deviced a system with IC–shift register for time delay.[4)]

In our laboratory, the recording system with a magnetic drum for time delay has been devised, being controlled by trigger and starter circuits for driving FM magnetic data recorders. The block diagram of this system is illustrated in Fig. 1. The

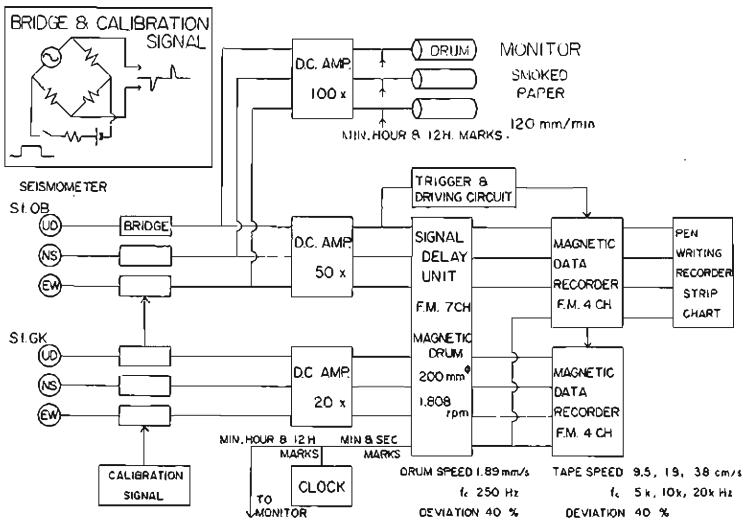

Fig. 1. Block diagram of observational system.

magnetic drum recorder can generate time delays of 30 sec, and the frequency range upto 25 Hz can be recorded. It has the advantage of having stability for a long time without a drop of SN ratio (about 42 db), since the drum head is untouched on its surface and thus free from mechanical wear. On the other hand, its disadvantage is in that signals are disturbed by shock motions and that moving of the instrument is difficult. Accordingly this equipment can not be used for recording of strong motions and field observations.

The sensing instruments are 3-components set of short period velocity seismometers having a natural period of 1.0 sec, damping ratio of 0.64 critical and sensitivity of 3 volts/kines. The output signals from each seismometer are connected to the recording system through amplifiers. The amplification factors are shown in Fig. 1. The recording sensitivity at the rock site is adjusted to 2.5 times higher than that at the ground site. The overall instruments response is shown in Fig. 2.

The seismic data in analog form on magnetic tape are converted to digital form through a high speed A–D converter and filed on a digital disk pack and magnetic tapes in a proper format to search and analyze necessary data using a computer (FACOM 230-25). The sampling interval of digital data is 0.01 sec in the case of near-distance events (S–P$<$9 sec) through a low-pass filter with a corner frequency of 25 Hz and attenuation rate of 30 db/oct, and 0.02 sec in the case of farther-distance events (S–P$>$9 sec) through low-pass filter with a corner of 10 Hz.

3. Observational points and geological conditions

The observational point on ground (GK in Fig. 3) has been set up at Uji-champus of Kyoto University located on the south-eastern side of the Kyoto basin

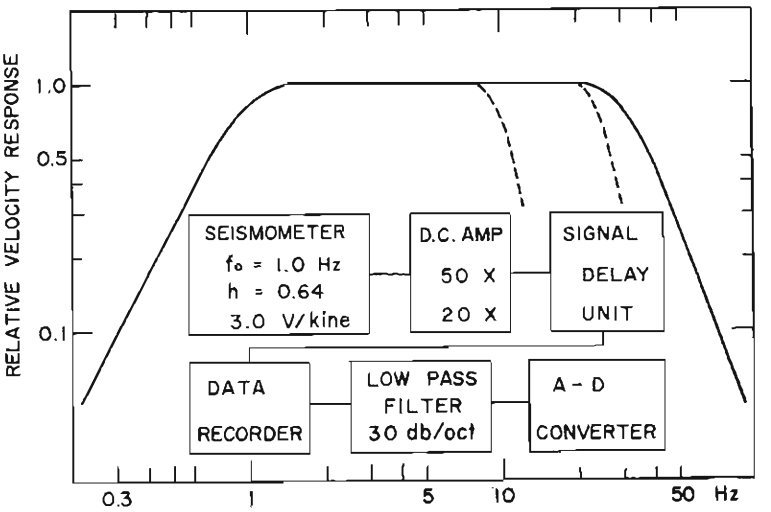

Fig. 2. Overall instrumental response curve. Dotted lines represent frequency response of 25Hz and 10Hz low pass filters used at A–D conversion.

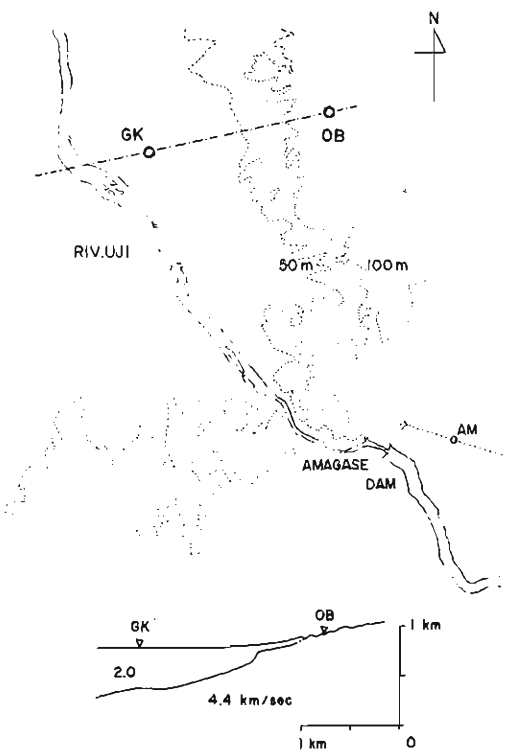

Fig. 3. Locations of observational points (GK and OB) and vertical profile along GK-OB line.

and that on rock (OB in Fig. 3) is on an outcrop halfway up a hill, Gounho, to the east of the ground site. The map of the vicinity of the two sites and the underground profile from east to west are shown in Fig. 3. The profile is based on data of seismic prospecting by means of refraction method of P waves.[5] Soil deposits in this area are reported to be formed of alluvium and diluvium, underlaid with bed rock which dips from east to west. Surface outcrops on the hill are reported to be formed of paleozoic strata.

The epicenters of analyzed events (observed from October, 1973 until June, 1974) are shown in Fig. 4 and the examples of seismograms at the rock site and the ground site are shown in Fig. 5.

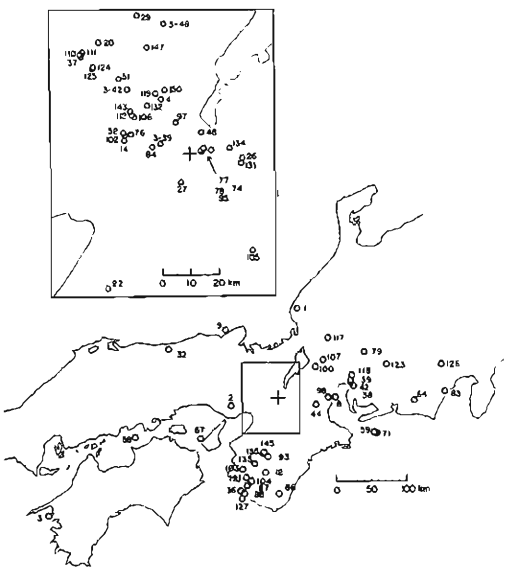

Fig. 4. Locations of epicenters of analyzed events.

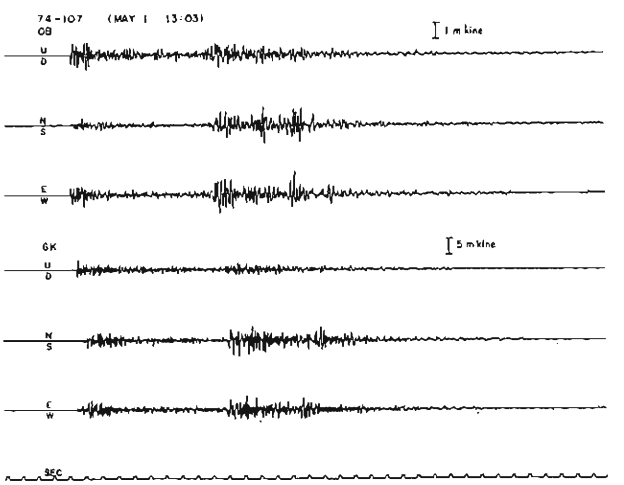

Fig. 5. Examples of observed seismograms. Upper three traces show seismograms at rock (St. OB), and lower three, at ground (St. GK).

The arrival times of P waves at the ground site are considered to be delayed in comparison with those at the rock site because of low velocity of soil deposits. And so the spatial profile of the deposits in the vicinity of the ground site is examined from the differences of P onsets between the ground site and the rock site. In Fig. 6, the differences of P onsets between OB and GK site are plotted in epicentral directions. Solid circles show delay of P onsets at GK site to those at OB site, open circles show lead of P onsets at GK site and distance from the center to each circle shows the difference of P onsets between the two sites.

When seismic waves arrive from the east side (hill side in Fig. 3), P onsets at GK site are delayed 0.2~0.5 sec to those at OB site. P onsets at GK site are delayed 0.1~0.2 sec in the case of arrival from north-west to north, too. On the other hand, earlier arriving of P onsets at GK site is limited to the case of arrivals from north-west to southwest and the times in the lead are 0.18 sec at maximum.

The theoretical curves of delay and lead of P waves at GK site due to the deposit are shown in Fig. 6, using the schematic model simplified the underground profile shown in Fig. 3. The incident angle of P wave is assumed to be 45°. This value is found to be applicable to seismic waves from events of $t_{s-p}>8$ sec when particle motion diagrams of P waves at rock site in the vertical plane are examined as shown at later section. In Fig. 6 close agreement between the observed and calculated value is seen in the case of the arrivals from the area of east side and from the area of north-west to south-west.

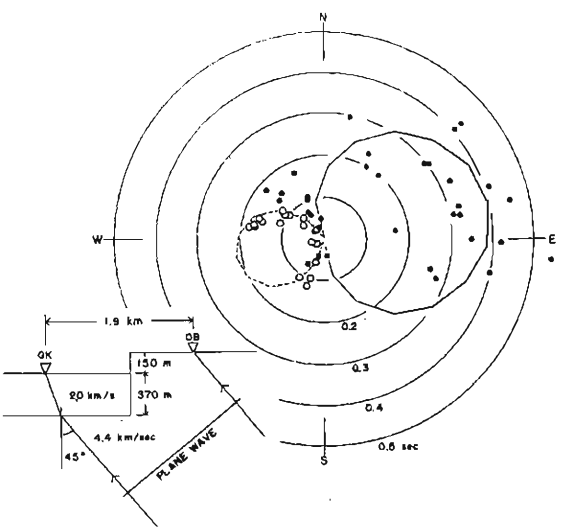

Fig. 6. Differences of P onsets between rock and ground site. Solid circles show delay of P onsets at GK site (ground) and open circles show lead. Direction and distance from center to each circle show epicentral direction and difference of P onsets between the two site. Solid and dotted line show theoretical delay and lead at GK, calculated using simplified model shown lower left.

However, P waves from the area of north-west to north arive at OB site earlier than at GK site, contrary to the theoretical expectation. This shows that the seismic waves from northly directions deflect to east, i.e., to hill side, in the vicinity of these sites. It is difficult to determine from this data whether this is due to the spatial profile of the deposits or to heterogeneity of rock. This is discussed in next section from data of particle motion diagrams at the rock site.

4. Particle motions

The natures of particle motions at the rock site and the ground site are examined to see variation of wave forms of P and S waves affected by local geology and topography. An example of seismograms at the rock site and the particle motion diagrams in the horizontal and vertical planes for four different frequency bands are shown in Fig. 7. The arrow indicates the epicentral direction (N44°W). The directions of particle motions of P waves are deflected to east side from the epicentral direction. The higher the frequency components are, the larger the deflection becomes. The directions of the particle motions of S waves are found to be different in different frequency bands. The orbital motions of S waves in the frequency band of less than 3Hz show the natures of the polarization of SV and SH waves corresponding to the epicentral direction.

The particle motions of P waves at the ground site show that P waves are nearly vertically incident to ground surface. And thus it is difficult to estimate the incident

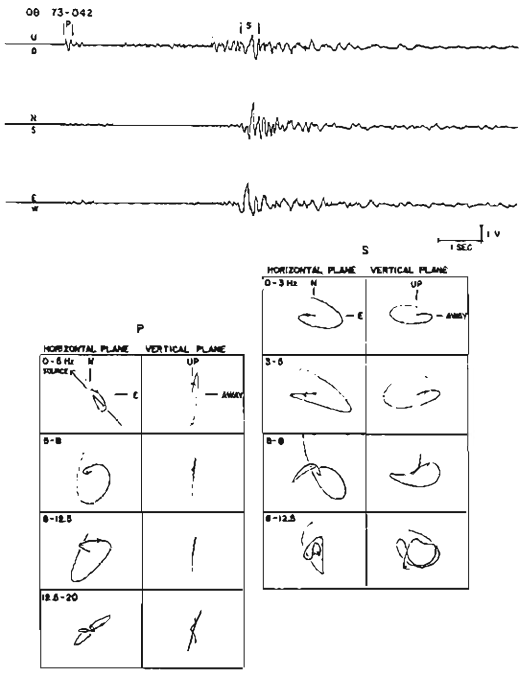

Fig. 7. Example of seismograms and particle motion diagrams in the horizontal and vertical planes for 4 different frequency bands.

azimuth from the particle motion diagrams in the horizontal plane because the amplitudes of the horizontal components of initial phases of P waves are very small.

In order to estimate an amplification factor of S waves at the ground from comparison of the amplitudes between the ground site and the rock site, it is necessary to separate SH and SV waves at the respective sites. However it is seen that the horizontal polarizations of S waves are different between the two sites from comparison of the particle motion diagrams of S waves. This is considered to be caused by horizontal heterogeneity of local geology. The nature of the polarization of seismic waves should be examined in detail to obtain an accurate amplification.

4-1 Deflection of directions of particle motions in the horizontal plane

The relation of the particle motions of P waves at the rock site to the epicentral directions is shown in Fig. 8 using 5 Hz-low-pass filtered seismograms. The horizontal directions of P initial motions from the area of north-west to north-east are deflected clockwise 30°~40° from the epicentral directions and on the other hand those from the area of south-west to south are counterclockwise 0°~20°. The particle motions at the rock site are affected by topographical features such as an inclination of the surface, as the rock site is on the side of a hill. The slope is within 15° as shown in Fig. 3. When the surface is assumed to be inclined at 15°, the deflection of the direction of the particle motion in the horizontal plane from the epicentral direction is about 3° at maximum in theoretical estimation using a half space model. The deflections in the observed particle motions are excessively large in comparison with those calculated. Thus the polarizations of initial motions of P waves shown in Fig. 8 should be considered to show that seismic waves incident to the site are deflected to hill side.

This nature of particle motions of P waves coincides with the deflection of the direction of P arrivals in the vicinity of this area inferred from the azimuthal variations

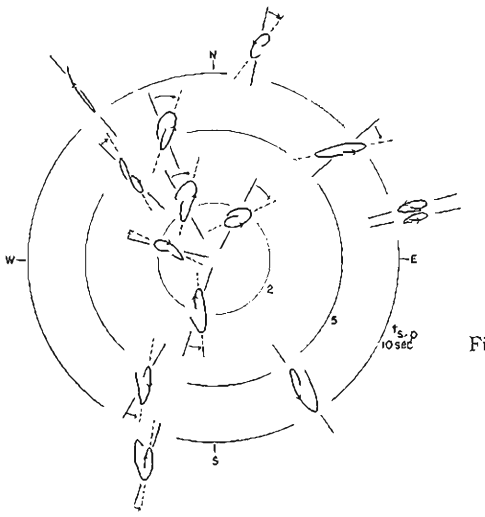

Fig. 8. Deflection of directions of P waves' particle motions in the horizontal plane from epicentral directions (solid line).

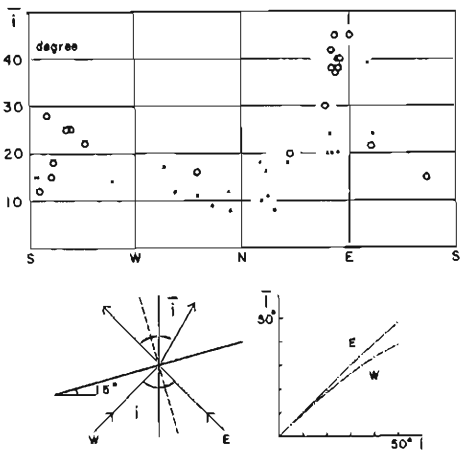

Fig. 9. Upper: azimuthal variation of apparent angles of incidence determined from particle motions of P waves in the vertical plane. Open circles and solid circles show apparent angles of incidence from events of $t_{s-p}>8$ sec and from events of $t_{s-p}<8$ sec, respectively.
Lower: effects of slope of rock surface to apparent angles of incidence calculated from half space model with dipping surface. i: True incident angles, $\bar{i}$: apparent angles of incidence. Dip angle of slope of rock surface is assumed to be 15°.

of the difference between P onset times at the rock site and the ground site abovementioned.

4–2 The azimuthal variation of particle motions in the vertical plane

The apparent angles of incidence of P waves are evaluated from particle motions diagrams in the vertical plane when the horizontal motions are divided into radial and transverse using the direction of P arrival. The relation between the apparent angles and the epicentral directions is shown in Fig. 9. Open circles and solid circles show the apparent angles of P waves from the events of $t_{s-p}>8$ sec and from the events of $t_{s-p}<8$ sec, respectively. In the case of further-distance events ($t_{s-p}>8$ sec), the apparent angles of incidence of P waves arriving from the east side are obtained at 30°～45° degrees while on the other hand, those from west side are obtained at 10°～30° degrees. In the case of near-distance events ($t_{s-p}<8$ sec), the apparent angles from east side are about 20° and those from west side are about 10°.

The incident angles of P waves are generally determined by focal depth and propagation path. The incident angles of seismic waves from near-distance events vary significantly dependent on focal depth and distance, but those from further-distance events might only slightly vary as long as the sources are within crust.

The apparent velocities of the further-distance events analyzed here are estimated to be 5.8～6.2 km/sec in the both cases from east side and west side by means of the curves of travel times of P onsets obtained at the micro-earthquake observation net of Abuyama Observatory. The incident angles of 42～52 degrees are estimated from the apparent velocities and the average velocity of P waves, about 4.6 km/sec, in this area, and the dependency of incident angles on the directions of the arrivals is not clear.

The effects of slope of the rock surface to the apparent angles of incidence must be considered as one of the causes of the systematic variation dependent on the azimuth shown in Fig. 9. When the dip angle of the rock surface is assumed to be 15° and

the ratio of P to S velocity, 2.0, the relation between the true incident angles and the apparent ones may be calculated for the simplified model as shown in Fig. 9. In the case of the incident angle of 50°, the apparent angles are about 45° for P wave from the east side and about 35° for that from the west side. Therefore, there are difference of about 10 degrees between the apparent angles of incidence for the waves arriving from opposite directions with the same incident angle. However the azimuthal variations of the apparent angles obtained from the particle motion diagrams in the vertical plane are above 2 times larger than the calculated value. In particular, the observed angles of P waves from the west side, i.e. ground side, (about 20 degrees), are considerably small when compared with the calculated value, (about 35 degrees). The observed ones from east side, i.e. hill side, are comparable with the calculated ones. Thus the variation of apparent angle is considered to be due in part to the effect of sloping rock surface and in addition to the effects of topographical reliefs of the hill and propagation path. The azimuthal characteristics of particle motions should be considered in estimating the amplification characteristics of the ground by comparing the seismic motion at the rock site with those at the ground site.

5. Comparison of earthquake motions at the rock site and at the ground site

5–1 Spectral characteristics of rock motions

The earthquake motions on a rock surface are generally considered to contain the features attributable to the effects of source and propagation path rather than the effects of near surface geology. But in the present case, the effects of the rock site on motions may be necessary to be examined since the site is on an outcrop halfway up a mountain where near surface geology is not so simple. On the other hand, the ground motions are generally considered to be significantly affected by near surface geological effects since the motions may be amplified by multiple reflections of P and S waves in the deposit layers.

In order to evaluate amplification factors of ground motions, the problem of estimating the characteristics of input motions to base rock below the ground from the data at the rock site should be discussed. The wavelets of initial parts of P and S waves are considered to be less disturbed by reflection and scattering from irregularity of rock than those of later parts. So, in order to estimate the spectral characteristics of input motions at the rock site, the amplitudes of initial parts of P and S waves are read as a function of frequency from filtered seismograms through various narrow frequency bands. The method of this analysis is shown by Fig. 10. The spectra of P and S waves are obtained by reading the amplitude of the wavelet indicated by dotted mark in each seismogram. Amplitude response of each band-pass-filter used here is shown in the left bottom and an example of P and S spectra is shown in the right bottom.

The predominant frequencies of vertical components of P waves and of NS and EW components of S waves obtained by this method are plotted as a function of magni-

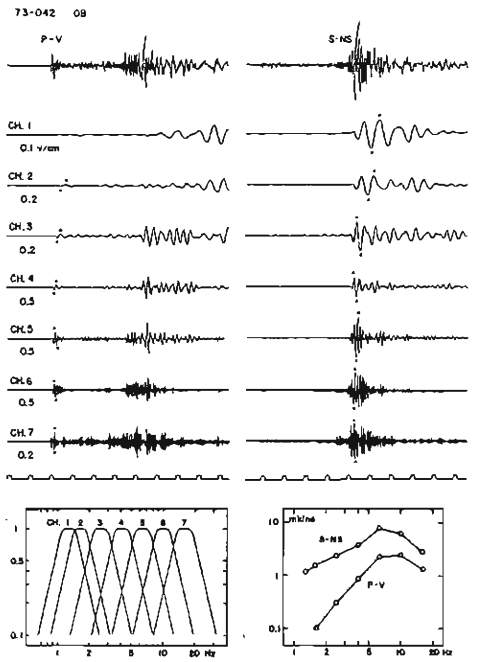

Fig. 10. Filtered seismograms through various narrow frequency bands. Spectra of P and S waves are obtained by readign amplitude of wavelet indicated by dots. Amplitude response of each band-pass-filter is shown in the left bottom.

tudes, as shown by Fig. 11. The predominant frequencies of P waves vary, relating to magnitudes and focal distances although there are some scatters. And those of S waves trend to vary with magnitudes and focal distances, but many of the predominant frequencies are 4∼5 Hz. The site effects of dominating at 4∼5 Hz should be considered in the case of horizontal motions of S waves at the rock site.

5-2 Amplification factors of ground motions

In order to evaluate amplification factors of earthquake motions at the ground site, amplitude ratios of P and S waves at the ground site to those at the rock site are obtained as a function of frequency using narrow-band-pass filtered seismograms. The amplitudes of ground motions are obtained by the same procedure as that for rock motions above-mentioned.

The ratios of P waves show a factor of about 2 in the frequency range lower than 2 Hz, but show variant amounts between about 0.8 and 8.0 in the higher frequencies. The higher the frequencies are, the larger is the variance. The ratios of S waves are variant between 0.8 and 8.0 in every frequency range. The amplifications at the ground site obtained in this method vary by a factor of about 10 times from event to event.

To examine the possible cause of the variation, the relation of the amplitude ratios to the azimuths of the seismic arrival and the apparent angles of incidence is discussed. In the right side of Fig. 13, the variation of the amplitude ratios of P waves with the

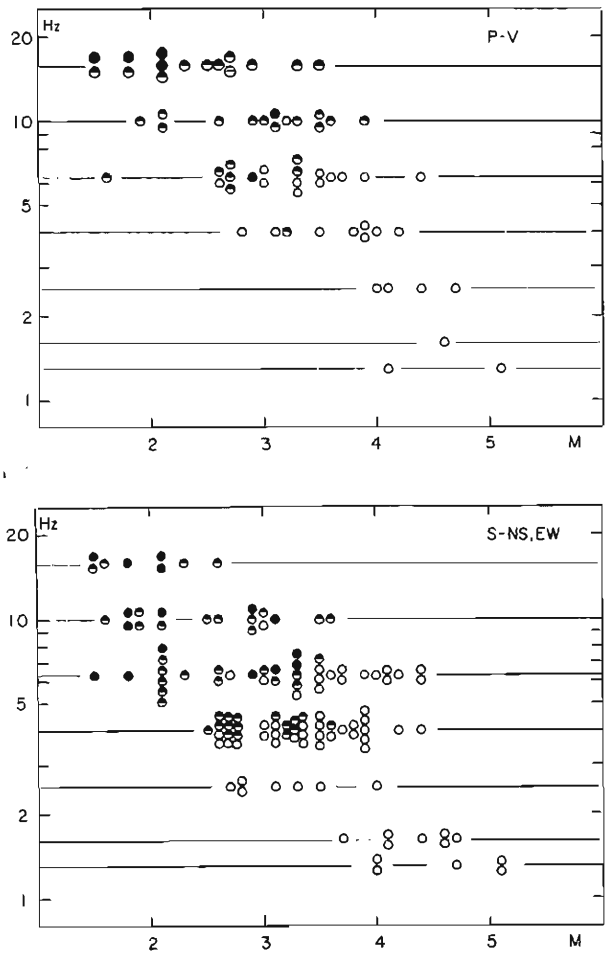

Fig. 11. Predominant frequencies of vertical components of P waves and of NS and EW components of S waves obtained in the method shown by Fig. 10.
● : $t_{s-p}<2$ sec, ◓ : $2<t_{s-p}<8$ sec, ○ : $t_{s-p}<8$ sec.

apparent angle of incidence is plotted for various frequency bands. The ratios tend to increase, as the apparent angles become larger. This becomes clearer in higher frequency ranges. In the left side of Fig. 13, the variation of the ratios with the azimuths of the arrivals is plotted. The ratios are significantly larger for the arrivals from the east i.e. the hill side, than for the arrivals from the other direction.

The systematic variations of the amplitude ratios seen in this figure may be either due to the site effects on the rock or due to the amplification effects on the ground. The apparent angles of incidence obtained at the rock are larger for the directions of the arrivals from the hill side than for the other direction as shown in Fig. 9. This shows that the dependence of the ratios on the apparent angle of incidence has the same

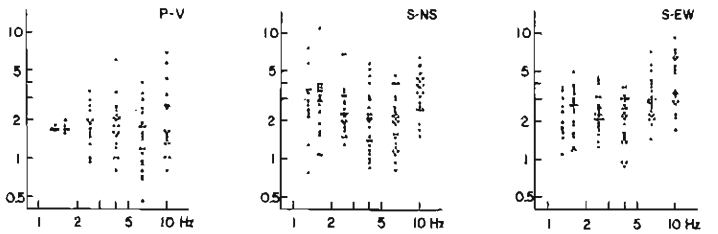

Fig. 12. Amplitude ratios of P and S waves at ground site to those at rock site obtained as a function of frequency using narrow-band-pass filtered seismograms. The pass bands are shown in Fig. 10.

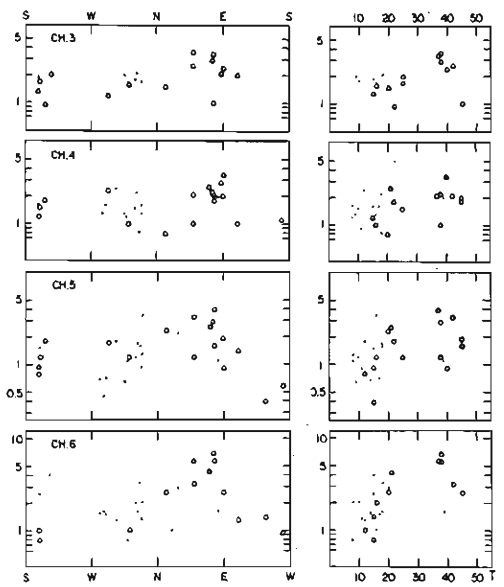

Fig. 13. Right: variation of amplitude ratios of P waves with apparent angles of incidence. Left: variation of amplitude ratios of P waves with epicentral direction. The pass band of each channel is shown in Fig. 10.

physical meaning as the dependence of the ratios on the azimuth. And then the azimuthal variations of the amplitude ratios are considered to be seriously influenced by the site effects on the rock. That is, the amplitudes of vertical components of P waves at the rock vary with the incident angles and, on the other hand, those at the ground are hardly influenced by the incident angle.

To interpret the site effects on the rock in detail, the observation at other points on the rock should be carried out to determine the azimuth of seismic arrival, the incident angle, the extent to where the same motions are obtained and the response at each point.

The relation of S waves' ratios to the azimuth does not show so clear systematic variation as compared with the case of P waves. This is partly due to difficulties of separation of SV and SH phases and partly due to contamination of later phases of P waves and converted waves. To obtain amplification factors of S waves, it is necessary

to discuss the separation of various phases by examining the differences of the polarizations of seismic motions between each site.

6. Comparison of Fourier spetcra at the rock site and the ground site

Comparison of Fourier spectra of P and S waves at the ground and the rock sites has been made to examine the amplification factors in the frequency components lower than 4 Hz. Wavelengths in this frequency range are comparable to the thickness of the deposits beneath the ground. For the present computation of spectra, the length of time window is 2.56 sec for P waves and 5.12 sec for S waves. The spectra of P waves at the rock and at the ground are shown by thin and thick curves, respectively, in Fig. 14. The event No. 74-133 was a shallow earthquake occurring near Wakayama and arrives from the ground side. No. 74-107 was a shallow earthquake near Gifu and arrived from the hill side. The spectrum of No. 74-133 at the rock shows a comparatively simple shape having a peak at 2.5 Hz and that at the ground has a peak at 2.0 Hz. The lowest peak frequency at the ground shifts to a lower frequency than that at the rock.

On the other hand, the spectrum of No. 74-107 at the rock shows trough in the range from 1.5 Hz to 4.0 Hz with remarkable peaks at 1.5 Hz and 4.0 Hz while that at the ground shows a smooth shape with a slight maximum of about 3 Hz in this frequency range. In the lower figure, the spectral ratios between these sites are shown. The theoretical curves are calculated from an analytic model of flat layers, the physical parameters of which are assumed, based on the data of refraction method for P waves and of well logging of P and S waves beneath to a depth of 50 m as shown in Table 1.

In the case of No. 74-133, the theoretical and observed curves are in comparatively good agreement over the low frequency range of interest. But in the case of No. 74-107, the peak frequency in the observed curves is higher and the peak amplitude is about

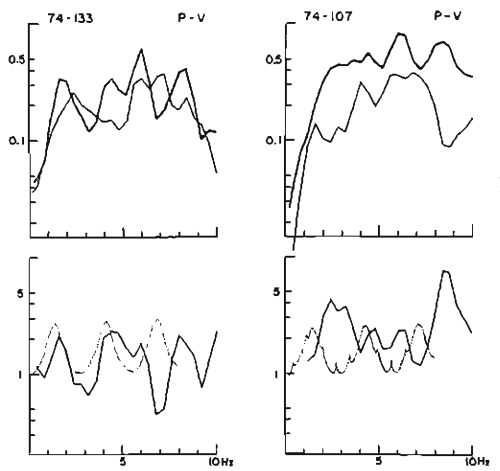

Fig. 14. Fourier spectra of P waves at rock site, thin line, and those at ground site, thick line. No. 74-107; epicenter, near Gifu, $t_{S-P}=8.9$ sec, arriving from hill side, No. 74-133; epicenter, near Wakayama, $t_{S-P}=12.7$ sec, arriving from ground site. Lower: spectral ratios between ground site and rock site. Dotted lines show theoretical curves calculated from analytic model with flat layers.

Table I Layered model at the ground in the calculation of Figure 14 and 16. The values are determined by means of experimental measurements such as seismic prospecting and seismic well logging, except for the values in parenthesis.

Thickness(m)	P Velocity (m/sec)	S Velocity (m/sec)	Density (g/cm^3)
3	1400	250	1.7
12	2100	440	(1.8)
6	1600	320	(1.8)
11	2200	580	(1.9)
8	1700	460	(1.9)
330	2000	580	(2.0)
	4400	(2400)	(2.5)

2 times larger than the calculated values. The lowest peak frequencies and the peak amplitudes of the spectral ratios are plotted as a function of the epicentral directions in Fig. 15. In the case of the arrivals from the ground side (west side), many of the spectral ratios have a peak around 2 Hz while on the other hand, in the case from the hill side (east side) there is a peak around 3 Hz. The peak amplitudes are larger in the case from the hill side than in the case from the other directions. The spectra of P waves observed at the rock site show a comparatively smooth shape between 1 Hz and 3 Hz in many cases and so the significant peaks seen in the spectral ratios may be mainly affected by amplification effects due to the deposit layers. The difference between the peak frequencies of the spectral ratios from hill side and those from the other side can not be explained by the response due to flat layers. Thus the effects of topographic features of the base rock beneath the deposits on the seismic waves should be considered. The azimuthal variation of the peak amplitudes of the ratio corresponds to those of the site effects at the rock which show the azimuthal variation of the apparent angles of incidence (§4.2).

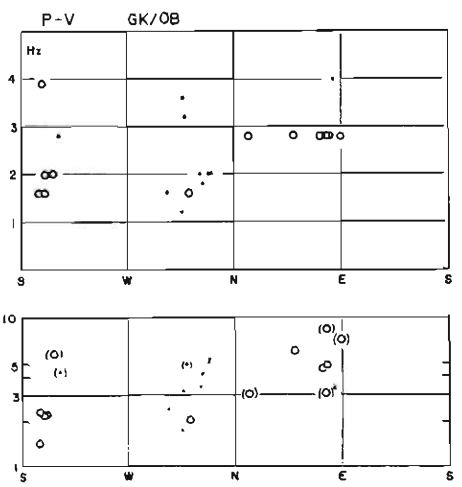

Fig. 15. Lowest peak frequencies (upper figure) and peak amplitude (lower figure) of spectral ratio of P waves between ground site and rock site as a function of epicentral direction. ○ : $t_{S-P}>8$ sec, ● : $t_{S-P}>8$ sec.

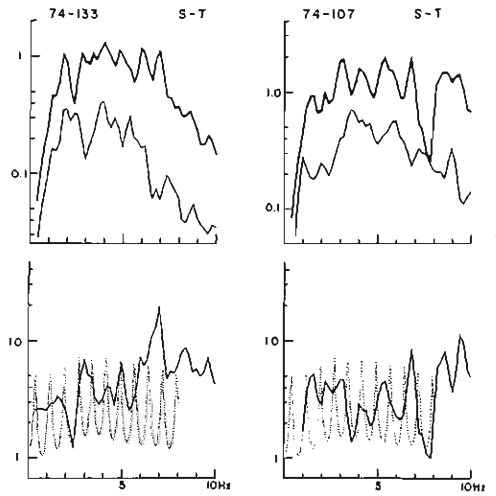

Fig. 16. Upper: Fourier spectra of S waves at rock site, thin line, and those at ground site, thick line. Lower: spectral ratios between ground site and rock site. Dotted lines show theoretical curves calculated from analytic model of flat layers.

The spectra of transverse components of S waves are shown in the upper graphs of Fig. 16 and the spectral ratios are shown together with the theoretical curve in the lower graphs of Fig. 16. It can be seen that the observed and theoretical curves of spectral ratios of S waves are different in both cases. This is partly due to uncertainties in assuming the S waves' velocity of each layer in calculation of theoretical curves and partly due to difficulties in correspondence of the same phases of seismic waves at the ground and at the rock.

The lowest peak frequencies and the peak amplitudes of the spectral ratios of S waves are plotted as a function of the epicentral directions in Fig. 17. The peak frequencies and amplitudes of the ratios from the hill side are found to be higher and larger than those from the other side, although its trend is not so clear as compared with the case of P waves.

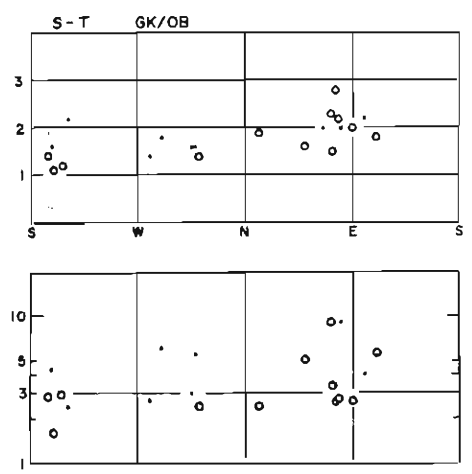

Fig. 17. Lowest peak frequencies (upper figure) and peak amplitudes (lower figure) of spectral ratio of S waves between ground site and rock site as a function of epicentral direction. ○ : $t_{s-p}>8$ sec, ● : $t_{s-p}<8$ sec.

The characteristics of the spectral ratios of P waves and S waves show that the effects due to the topographic features of the base rock under the ground have to be discussed to determine the amplification characteristics of the ground. At the same time, examination of the local effects at the rock site is necessary to determine the variation in the amplification factors observed.

7. Conclusion

Some problems in estimating the amplification factors of ground motions during earthquakes are indicated from a comparison of earthquake motions observed at the rock site with those at the ground site. The seismic motions at the rock site are characterized by the effects of local geology, dependent on the directions of seismic arrivals, as well as by the effects due to magnitudes and focal distances. The amplitude ratios of P and S motions at the ground to those at the rock show appreciable variations of factors from 0.8 to 8.0 from event to event. The spectral ratios between the ground motions and the rock motions show that the frequencies and amplitudes of the peaks are different, dependent on the incident direction of the seismic waves.

These are considered to be caused by the local conditions both at the rock site and at the ground site. The causes of the variation of the amplitude ratios is found to be that the amplitude of the motions at the rock site, on the hill, vary with the incident angles and the directions of seismic arrivals. While the peak frequencies of the responses of seismic motions at the ground site, underlied by dipped base rock, are considered to vary with the direction of seismic arrivals.

This is found to be significant in the case of P waves but not so clear in the case of S waves because of large scatter. This is due to difficulty in separating and comparing SH and SV waves at each site, because polarization of S motions are different between the two sites.

These observational facts show that the evaluation of the amplification factors using only a small amount of data will result in inaccuracy, particularly in the case of complex local geology in the vicinity of a given site.

In future, a suitable net of the observation points should be deployed to obtain the input motions to the base rock and to evaluate the amplification factors of the ground motions.

Acknowledgements

The authors wish to express their sincere thanks to Prof. Soji Yoshikawa for his encouragement and also to Mr. Tamotsu Furuzawa of Kyoto University for his valuable discussion in carrying out this work.

The data processing was run on a Facom 230–25 at the Information Data Processing Center for Disaster Prevention Research, of the Disaster Prevention Research Institute of Kyoto University and the numerical computations were run on a Facom 230–75 at the Data Processing Center of Kyoto University.

References

1) Murphy, J. R., A. H. Davis and N. L. Weaver: Amplification of Seismic Body Waves by Low-velocity Surface Layers, Bull. Seism. Soc. Am., Vol. 61, 1971, pp. 109–145.
2) Davis, L. L. and L. R. West: Observed Effects of Topography on Ground Motion, Bull. Seism. Soc. Am., Vol. 63, 1973, pp. 283–298.
3) Irikura, K., J. Akamatsu and T. Furuzawa: Some Problems in Determining Earthquake Ground Motions on Base Rock, Proc. Fifth World Cont. on Earthq. Eng., June, 1973.
4) Furuzawa, T.: Some Problems of Seismic Data Processing. Part 1. Observational System and Instrumentation. Bull. Disas. Prev. Res. Inst., Kyoto Univ., Vol. 24, 1974, pp. 49–66.
5) Kitsunezaki, C., N. Goto and T. Iwasaki: Underground Structure of the Southern Part of the Kyoto Basin Obtained from Seismic Exploration and Some Related Problems of Earthquake Enginnering, Annuals, Disast. Prev. Res. Inst. No. 14A, 1971, pp. 203–217.
6) Haskell, N.: Crustal reflection of plane P and SV waves, J. Geopys. Res., Vol. 67, 1962, pp. 4751–4767.